

11-2-2023

Doxorubicin-Induced Modulation of TGF- β Signaling Cascade in Mouse Fibroblasts: Insights into Cardiotoxicity Mechanisms

Conner Patricelli
Boise State University

Parker Lehmann
Idaho College of Osteopathic Medicine

Julia Thom Oxford
Boise State University

Xinzhu Pu
Boise State University

Publication Information

Patricelli, Conner; Lehmann, Parker; Oxford, Julia Thom; and Pu, Xinzhu. (2023). "Doxorubicin-Induced Modulation of TGF- β Signaling Cascade in Mouse Fibroblasts: Insights into Cardiotoxicity Mechanisms". *Scientific Reports*, 13, 18944. <https://doi.org/10.1038/s41598-023-46216-7>



OPEN Doxorubicin-induced modulation of TGF- β signaling cascade in mouse fibroblasts: insights into cardiotoxicity mechanisms

Conner Patricelli¹, Parker Lehmann², Julia Thom Oxford^{1,3,4} & Xinzhu Pu^{3,4}✉

Doxorubicin (DOX)-induced cardiotoxicity has been widely observed, yet the specific impact on cardiac fibroblasts is not fully understood. Additionally, the modulation of the transforming growth factor beta (TGF- β) signaling pathway by DOX remains to be fully elucidated. This study investigated DOX's ability to modulate the expression of genes and proteins involved in the TGF- β signaling cascade in mouse fibroblasts from two sources by assessing the impact of DOX treatment on TGF- β inducible expression of pivotal genes and proteins within fibroblasts. Mouse embryonic fibroblasts (NIH3T3) and mouse primary cardiac fibroblasts (CFs) were treated with DOX in the presence of TGF- β 1 to assess changes in protein levels by western blot and changes in mRNA levels by quantitative reverse transcriptase polymerase chain reaction (qRT-PCR). Our results revealed a dose-dependent reduction in cellular communication network factor 2 (CCN2) protein levels upon DOX treatment in both NIH3T3 and CFs, suggesting an antifibrotic activity by DOX in these fibroblasts. However, DOX only inhibited the TGF- β 1 induced expression of COL1 in NIH3T3 cells but not in CFs. In addition, we observed that DOX treatment reduced the expression of BMP1 in NIH3T3 but not primary cardiac fibroblasts. No significant changes in SMAD2 protein expression and phosphorylation in either cells were observed after DOX treatment. Finally, DOX inhibited the expression of Atf4 gene and increased the expression of Cdkn1a, Id1, Id2, Runx1, Tgfb1, Inhba, Thbs1, Bmp1, and Stat1 genes in NIH3T3 cells but not CFs, indicating the potential for cell-specific responses to DOX and its modulation of the TGF- β signaling pathway.

Chemotherapy has improved cancer survival rates, however, side effects of chemotherapeutic drugs remain a concern. An increased risk of cardiovascular complications and cardiotoxicity is attributed to anthracyclines^{1–4}. Anthracyclines are a class of naturally occurring antibiotics produced by *Streptomyces* bacteria that exhibit broad anticancer efficacy. One of the most widely used anthracyclines is DOX, which was approved by the FDA in 1974 for the treatment of cancers, including hematopoietic cancers such as leukemias and lymphomas, and metastatic solid tumors such as breast, gastric, neuroblastoma, lung, ovarian, and bladder cancers in both adult and pediatric patients⁵.

DOX has been known to damage various types of cells in the heart, including cardiomyocytes, fibroblasts, and endothelial cells, which can lead to lethal cardiomyopathy^{6–9}. Echocardiography and cardiac magnetic resonance imaging are standard methods used to monitor the left ventricle ejection fraction (LVEF) to assess the progression of cardiotoxicity induced by DOX^{10–14}. DOX-induced cardiotoxicity is characterized by a gradual decline in LVEF which, if not managed, can lead to heart failure. A significant reduction in LVEF is defined as a decrease of more than 10% from baseline to a value below the lower limit of normal (usually less than 50–55%)^{14–16}. The risk of developing cardiotoxicity increases with the cumulative dose of DOX¹⁷. The reported risk of DOX-induced cardiotoxicity by cumulative dose is 3–5% for 400 mg/m², 7–26% for 550 mg/m², and 18–48% for 700 mg/m²^{18–22}. Moreover, age is a significant factor that contributes to the susceptibility to cardiotoxicity in DOX-treated patients. Patients under five years old or over sixty-five years old are more vulnerable to developing

¹Biomolecular Sciences Graduate Programs, Boise State University, Boise, ID 83725-1512, USA. ²Idaho College of Osteopathic Medicine, Meridian, ID 83642-8046, USA. ³Biomolecular Research Center, Boise State University, Boise, ID 83725-1511, USA. ⁴Department of Biological Sciences, Boise State University, Boise, ID 83725-1515, USA. ✉email: shinpu@boisestate.edu

cardiotoxicity^{18,23}. It is likely that these age groups are more prone to cardiotoxicity due to age-related differences in the cardiovascular system which also increase the risk of developing heart failure.

DOX exerts its antitumor activity by intercalating into DNA, which inhibits the binding of topoisomerase II β and the unwinding of supercoiled DNA^{24–27}. This inhibition leads to a blockage of DNA synthesis and the eventual induction of double-stranded DNA breaks, triggering programmed cell death in cells^{28,29}. In addition, DOX has been shown to induce cellular senescence in tumor and normal cells^{30–35}. Despite its therapeutic benefits, DOX is associated with off-target effects, which include the production of reactive oxygen species (ROS). The precise mechanisms underlying DOX-induced ROS production are not fully understood, however, studies suggest that mitochondrial dysfunction^{36,37}, calcium homeostasis^{38,39}, iron chelation^{40,41}, and inflammatory responses^{42–45} are implicated in ROS generation caused by DOX. Although antioxidants have been used in combination with DOX to decrease the buildup of free radicals, this approach has not proven effective in reducing cardiotoxicity while maintaining the antitumor efficacy of DOX⁴⁶.

The myocardium is a complex tissue comprising multiple cell types, including cardiac fibroblasts (CFs) and endothelial cells (ECs)⁴⁷. CFs and ECs play crucial roles in regulating the expression and accumulation of extracellular matrix (ECM) components such as collagens, fibronectin, matrix metalloproteinases (MMPs), and endogenous protease inhibitors known as tissue inhibitors of metalloproteinases (TIMPs)^{48–52}. Transforming growth factor β (TGF- β) is a pivotal cytokine/growth factor that has been shown to stimulate fibroblasts^{53,54}. The TGF- β signaling pathway has been implicated in fibrosis in the myocardium, which contributes to cardiac dysfunction^{55–59}. In this study, we investigated the effects of DOX on the TGF- β signaling cascade in mouse fibroblasts from two sources to better understand the mechanisms of its cardiotoxicity.

Results

Effect of DOX on fibroblast viability

Cell viability of NIH3T3 and CFs was evaluated using an alamarBlue assay. Cells were treated with 0 – 50 μ M DOX for 24 h. A significant decrease in cell viability was observed at 2.5 μ M DOX and above (Fig. 1).

DOX treatment inhibited CCN2 protein expression in a dose-dependent manner

Cellular communication network factor 2 (CCN2), formerly known as connective tissue growth factor (CTGF), is a matricellular protein involved in many cellular processes^{64,65}. To assess the impact of DOX on CCN2 in fibroblasts, we employed western blot techniques to evaluate CCN2 protein levels in NIH3T3 cells and CFs. The cells were exposed to increasing concentrations of DOX (0, 0.25, 1, or 2.5 μ M) in the presence and absence of TGF- β 1 stimulation, for 24 h. CCN2 protein expression in both NIH3T3 and CFs was stimulated by TGF- β 1 (Fig. 2). However, CFs showed a more robust constitutive expression of CCN2 than that of NIH3T3 in the absence of TGF- β 1. A dose-dependent downregulation of CCN2 protein expression was observed in both cell lines treated for 24 h with DOX (Fig. 2). These results suggest that DOX modulates the expression of CCN2 in fibroblasts and that DOX may play a role in ECM remodeling.

DOX treatment reduced the expression of BMP1 in NIH3T3 but not primary cardiac fibroblasts

BMP1 (Bone Morphogenetic Protein 1), a pivotal member of the astacin family of metalloproteinases, plays a central role in processing and maturing extracellular matrix components, particularly collagens⁸⁸. To investigate whether DOX's potential impact on BMP1 expression in fibroblasts, cells were treated with DOX at a concentration of 1 μ M for 24 h and BMP1 protein expression was assessed. DOX induced a significant decrease in BMP1 expression in NIH3T3 cells without the presence of TGF- β 1, but not in CFs (Fig. 3). These results suggest that DOX suppresses BMP1 protein expression in a cell dependent manner.

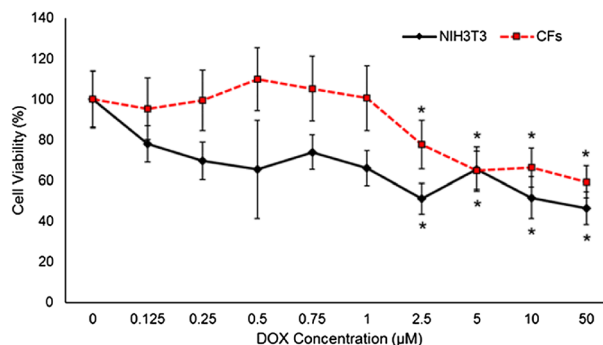


Figure 1. Cytotoxicity of DOX in primary cardiac fibroblast cells isolated from BALB/c mice and NIH3T3 embryonic fibroblast cell line. Cells were treated with series concentrations of DOX (0–50 μ M) for 24 h. Cell viability was assessed using the alamarBlue assay. Values represent mean \pm standard error ($n = 6$). * P -value < 0.05 compared to control (Student's t -test).

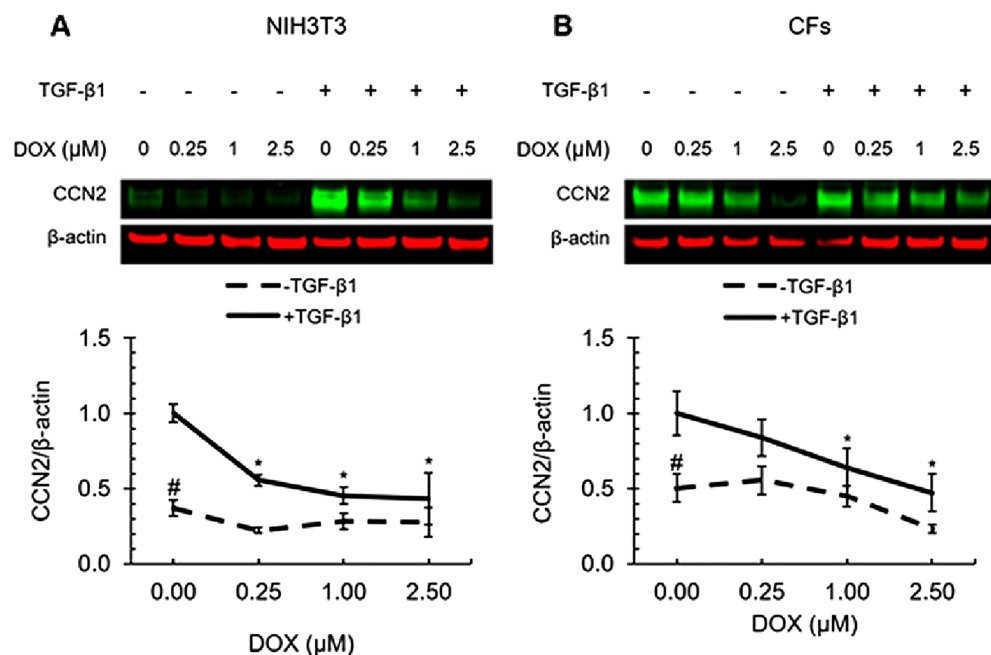


Figure 2. DOX inhibited CCN2 expression in a dose-dependent manner. Western blot analysis of the effects of DOX on CCN2 expression in NIH3T3 cells (A) and CFs (B). Densitometry results normalized to the treatment group with TGF- β 1 and without DOX. Values represent mean \pm standard error ($n=4$). * P -value < 0.05 compared to treatment group containing TGF- β 1 and lacking DOX (two-way ANOVA with Dunnett's test). # P -value < 0.05 compared to treatment group containing TGF- β 1 and lacking DOX (two-way ANOVA with Dunnett's test).

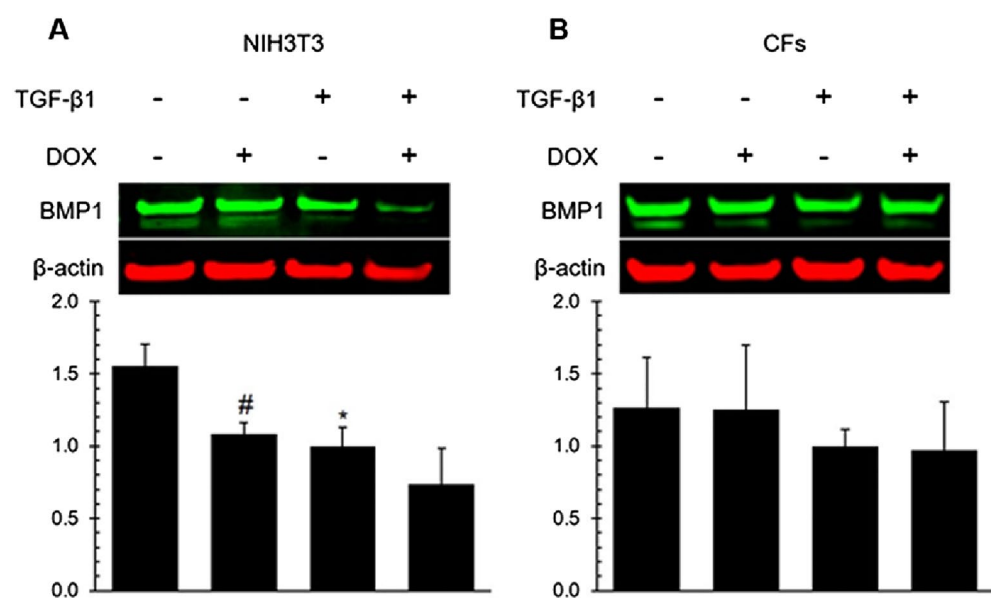


Figure 3. DOX significantly reduced BMP1 protein levels in NIH3T3 cells but not in CFs. Western blot analysis of the effect of DOX on BMP1 expression in NIH3T3 cells (A) and CFs (B). Densitometry results were normalized to the treatment group with TGF- β 1 and without DOX. Values represent mean \pm standard error ($n=3$). * P -value < 0.05 compared to the treatment group with TGF- β 1 and without DOX (Student's t -test). # P -value < 0.05 compared to the treatment without TGF- β 1 or DOX (Student's t -test).

DOX did not induce the phosphorylation of SMAD2 in NIH3T3 cells and CFs

To investigate whether DOX affects the activation of the TGF- β /SMAD2 signaling pathway, we assessed SMAD2 and pSMAD2 in NIH3T3 and CFs treated with TGF- β 1 and DOX for one hour. No significant changes in SMAD2 protein expression in either cells were observed after DOX treatment (Fig. 4). TGF- β 1 stimulation led to a significant increase in pSMAD2 in both cell lines, in agreement with previous findings⁶¹. DOX didn't induce significant changes in SMAD2 phosphorylation (Fig. 4).

DOX treatment inhibited the TGF- β -induced COL1 protein expression in NIH3T3 cells but not CFs

Collagen Type I (COL1) is a fundamental structural protein essential for maintaining tissue integrity and is predominantly secreted by fibroblasts^{57,85}. To assess the impact of DOX on COL1 protein expression in NIH3T3 cells and CFs, we conducted western blot analysis following a 24-h treatment with DOX and TGF- β 1. Our results revealed that TGF- β 1 treatment induced an increase in COL1 protein levels in NIH3T3 cells (Fig. 5). The presence of DOX effectively inhibited the TGF- β 1-induced expression of COL1 protein (Fig. 5). These findings suggest that DOX treatment exerts a suppressive effect on COL1 production, which may have implications for the deposition of mature collagen within the extracellular matrix surrounding cardiac fibroblasts.

DOX induced differential expression of genes in the TGF- β /BMP signaling pathway in NIH3T3 cells but not CFs

In this study, we examined the effects of DOX on the expression of genes in the TGF- β /BMP signaling pathway using qRT-PCR. DOX-induced differential expression of several genes in this pathway were observed in NIH3T3 cells, including upregulation of Id1, Id2, Runx1, Tgfb1, Inhba, Thbs1, Bmp1, and Stat1, and downregulation of Atf4 (Fig. 6, Table 1). In contrast, no significant gene alterations were observed in CFs under the same conditions (Supplementary Fig. 1). These findings indicate that DOX impacts TGF- β and BMP signaling in a cell type-specific manner.

Discussion

DOX is a widely used antibiotic with broad antitumor efficacy for treating hematopoietic and metastatic solid tumor cancers. However, its cardiotoxic side effect limits its clinical use. DOX-induced cardiotoxicity may manifest within hours of initial treatment and persist up to twenty years post-final administration, posing a potential lifelong risk for patients treated with DOX^{17–22}. Despite five decades of research, there is still no therapeutic option to reduce the risk of developing cardiotoxicity while maintaining its antitumor efficacy. While cardiomyocytes

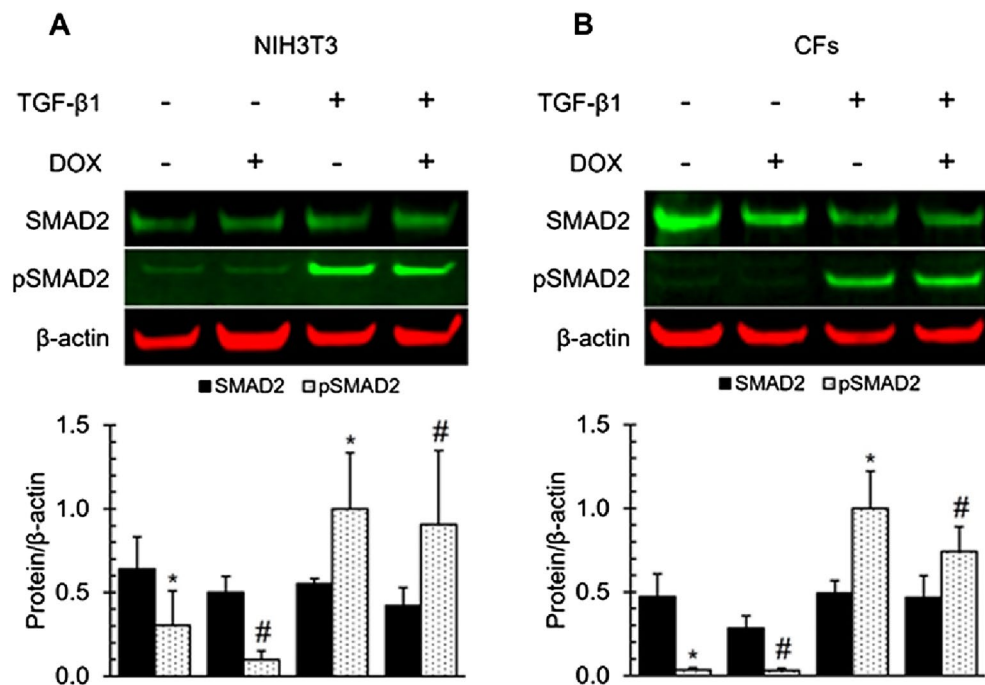


Figure 4. TGF- β 1 induced the phosphorylation of SMAD2 in both NIH3T3 cells and CFs. DOX treatments did not significantly effect SMAD2 or pSMAD2 in one hour. Western blot analysis of NIH3T3 cells (A) and CFs (B) probing SMAD2 and phosphorylated SMAD2. Densitometry was performed on SMAD2, pSMAD2, and normalized to housekeeping protein β -actin then normalized to pSMAD2 of the group treated with TGF- β 1 and without DOX. Values represent mean \pm standard error (n = 4). * *P*-value < 0.05 compared to normalized pSMAD2 (Student's *t*-test). #, *P*-value < 0.05 compared to treatments with DOX and with and without TGF- β 1 (Student's *t*-test).

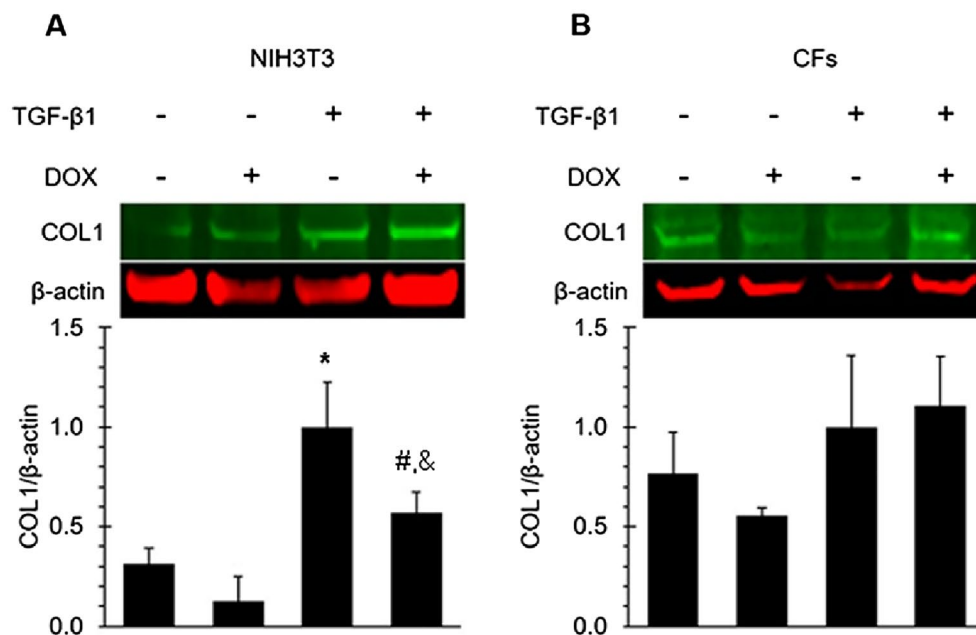


Figure 5. DOX inhibited the TGF- β 1 induced expression of COL1 in NIH3T3 cells but not in CFs. Western blot analysis of NIH3T3 cells (A) and CFs (B) probing COL1 protein levels with and without TGF- β 1 stimulation and DOX. Densitometry results were normalized to the treatment of TGF- β and without DOX. Values represent mean \pm standard error ($n=4$). *, P -value < 0.05 compared to treatment stimulated with TGF- β 1 without DOX (Student's t -test). #, P -value < 0.05 compared to treatment group stimulated with TGF- β 1 and DOX (Student's t -test).

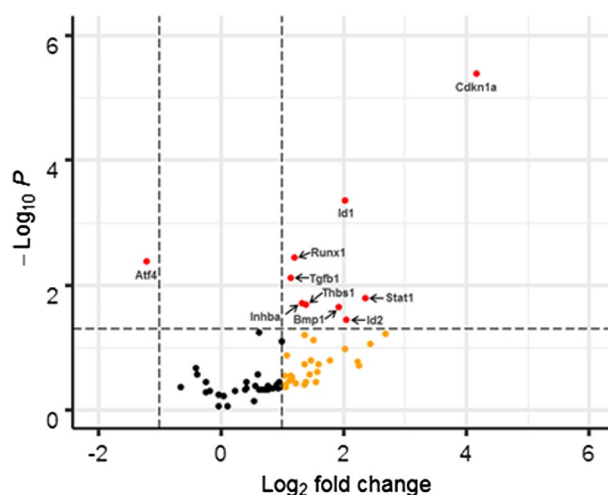


Figure 6. DOX inhibited the TGF- β 1 induced expression of Atf4 and increased the expression of Cdkn1a, Id1, Id2, Runx1, Thbs1, Tgfb1, and Stat1 in NIH3T3 cells. Cells were treated with 10 ng TGF- β 1 with or without 1 μ M DOX for 24 h. Experiments were performed in triplicates. Student's t -test with Bonferroni correction was used for statistical analysis.

are the cells within the myocardium responsible for the contraction of the heart, CFs, and vascular endothelial cells are responsible for the synthesis, deposition, and degradation of cardiac extracellular matrix (ECM) and play critical roles in maintaining normal functions of the heart^{62,63}.

In this study, we investigated and compared the effects of DOX on TGF- β signaling cascade in primary cardiac fibroblasts and NIH3T3 embryonic fibroblasts. We first examined the protein expression of CCN2 in the cells following DOX treatment. A dose-dependent downregulation of CCN2 protein expression was observed in both cells treated for 24 h with DOX. CCN2 is highly expressed during the organ development stage and its expression is limited during adulthood^{64,65}. The expression of CCN2 is greatly upregulated during the fibrogenic process, in which fibroblasts are activated^{64,65}. CCN2 expression was minimal in NIH3T3 without the treatment of TGF- β 1,

Gene symbol	Gene name	Alias	Regulation
Atf4	Activating transcription factor 4	Creb-2, Taxreb67, Txreb	Down
Bmp1	Bone morphogenetic protein 1	Bmp-1, Pcolc, Tolloid-like	Up
Cdkn1a	Cyclin dependent kinase inhibitor 1A	p21, Cap20, Cip1, Waf1, Sd1, p21cip1, cdkn1	Up
Id1	Inhibitor of DNA Binding 1	Bhlhb24	Up
Id2	Inhibitor of DNA Binding 2	Bhlhb26, Gig8	Up
Inhba	Inhibin subunit beta A	Edf, Activin beta-A chain	Up
Runx1	RUNX Family transcription factor 1	Amlcr1, Cbfa2, Aml1, Aml1/ETO, Pebp2a2	Up
Stat1	Signal transducer and activator of transcription 1	Stat91, Isgf-3	Up
Tgfb1	Transforming growth factor beta 1	Tgfbeta, Tgfb, Ced, Dpd1	Up
Thbs1	Thrombospondin 1	Tsp1, Tsp, Thbs-1, Tsp-1	Up

Table 1. Up/Downregulated Genes in NIH3T3 Cells Treated with DOX and TGF- β 1.

a known stimulator of CCN2^{64,66}. Interestingly, constitutive CCN2 was more robust in CFs, suggesting that CFs might have undergone activation. A similar observation was reported in primary hepatic stellate cells (HSCs)⁶⁷. A strong expression of CCN2 in HSCs was found and TGF- β 1 did not simulate CCN2 expression⁶⁷. These data suggest that constitutive expression of CCN2 and stimulation by TGF- β 1 may be cell-dependent.

CCN2 is a multifunctional matricellular protein involved in many biological processes, including ECM production, migration, differentiation, angiogenesis, and apoptosis^{68–70}. It is a central mediator of tissue remodeling and fibrosis⁷¹. CCN2 is upregulated during tissue remodeling and fibrogenesis. One of the chronic manifestations of DOX-induced cardiomyopathy is fibrosis in the myocardium. However, in our study, DOX was found to decrease CCN2 expression in both cell lines, which implicates an antifibrotic activity. This contradiction may result from differences in the length of exposure and underlying cellular responses induced by DOX. Though the mechanisms of fibrotic changes induced by DOX are not fully understood, it is believed fibrosis is caused by the death of cardiomyocytes induced by DOX via various mechanisms, which include oxidative stress, topoisomerase inhibition, ferroptosis, cardiogenetics, mitochondrial bio-energetics, and autophagy modulation^{72–80}. Direct regulation of fibrogenic signaling by DOX is not clear. In this study, cells were treated with DOX for 24 h. The observed decrease in CCN2 expression suggests that acute exposure may induce a different response in fibrotic signaling in fibroblasts. DOX has been reported to impair wound healing, reduce collagen production, and inhibit skin fibroblast proliferation^{81–84}. We further examined whether DOX-induced downregulation of CCN2 affects the expression of Collagen type I, which is the most abundant type of collagen and is a major structural component of the cardiac ECM^{85,86}. We observed that TGF- β 1 stimulated a significant increase in COL1 protein level in NIH3T3 cells. DOX treatment significantly suppressed TGF- β 1-induced COL1 upregulation. In contrast, similar effects were not observed in primary cardiac fibroblasts. Such differences between the two cells may result from distinct expression patterns of CCN2 in each cell. As discussed above, while CCN2 expression was minimal in NIH3T3 and was greatly stimulated by TGF- β 1, it was strongly expressed in CFs without the presence of TGF- β 1. This may have contributed to the different effects of DOX in the downstream expression of COL1.

BMP1 is involved in the regulation of TGF- β signaling pathway by cleaving the pro-domain of TGF- β precursors, which releases the active TGF- β ligand that then binds to its cell surface receptor complex and activates downstream SMAD proteins^{87,88}. In this study, we observed that DOX induced a significant decrease in BMP1 expression in NIH3T3 cells, but not in CFs (Fig. 3). These results suggest that DOX suppress BMP1 protein expression in a cell dependent manner.

SMAD proteins play an important role in TGF-mediated ECM gene expression and regulation. Phosphorylation of cytoplasmic mediators belonging to the SMAD family is needed for signaling from TGF- β type I receptor to the nucleus after ligand activation⁸⁹. In this study, we examined whether SMAD2 and BMP1 were involved in DOX-induced downregulation of CCN2 expression in fibroblasts primary cardiac fibroblast cells and NIH3T3 cells. TGF- β 1 induced a significant increase in SMAD2 phosphorylation as expected⁶¹. DOX did not affect SMAD2 protein expression and phosphorylation. These results indicate that SMAD2 played no significant roles in DOX-induced CCN2 downregulation observed in this study.

In addition, this study examined the effects of DOX on gene transcription in the TGF- β and BMP signaling pathways. Significant alterations in the expression of 10 genes were observed in NIH3T3 cells treated with DOX and TGF- β 1, however, no differential gene expression was observed in CFs under the same conditions. Specifically, we observed that activating transcription factor 4 (Atf4) was significantly downregulated in NIH3T3 cells treated with TGF- β 1 and DOX compared to TGF- β 1 treatment alone. Prior reports have indicated a positive correlation between ATF4 protein levels and the expression of COL1⁹⁰. These findings suggest a potential association between decreased expression of the Atf4 gene and reduced COL1 protein expression. This is further evidenced by the increased gene expression of Inhibitor of DNA binding 1 (Id1) and Runt-related Transcription Factor 1 (Runx1). Id1 is an inhibitor of the TGF- β -induced collagen synthesis⁹¹. RUNX1 has been demonstrated in various cancer studies to inactivate the TGF- β 1/SMAD signaling pathway which is also responsible for the deposition of collagen⁹².

Interestingly, there was an upregulation of Tgfb1, transforming growth factor beta 1, mRNA expression. This could be explained by the increase in Thbs1 mRNA which promotes Tgfb1 mRNA expression in fibroblasts⁹³.

Signal transducer and activator of transcription 1 (Stat1), a downstream target of the TGF- β signaling pathway, was upregulated in NIH3T3 cells upon treatment with DOX + TGF- β 1 compared to TGF- β 1 treatment alone. Stat1 has been observed to inhibit the myofibroblast phenotype in cells of fibroblastic origin *in vivo*⁹⁴. This would suggest that DOX prevents the transformation of fibroblasts to myofibroblasts. Lastly, we observed a significant upregulation of cyclin-dependent kinase inhibitor 1A (Cdkn1a) (also known as p21) in NIH3T3 cells following DOX treatment. Cdkn1a is a senescence marker for oxidative stress that induces G2 arrest in the cell cycle in human fibroblasts^{95–98}. DOX has been reported to induce a time-dependent increase of P21^{cip1/waf1} in cultured neonatal rat cardiomyocytes³⁵. DOX has also been shown to increase P21^{cip1/waf1} gene and protein expression in mouse liver and kidney *in vivo*⁹⁹.

In summary, the results from this study suggest that DOX treatment can modulate the expression of key genes involved in TGF- β signaling, ECM synthesis, and remodeling in fibroblasts in a cell origin dependently manner. Further investigations are warranted to elucidate the underlying mechanisms and functional implications of these observations.

Materials and methods

Cell culture

Cardiac fibroblasts (CFs) from BALB/c mice were purchased from Cell Biologics (Chicago, Illinois, USA) and cultured in fibroblast medium provided by the vendor, which contained 0.5 mL fibroblasts growth factor (0.1% v/v), 0.5 mL hydrocortisone (0.1% v/v), 5 mL 100 \times antibiotic–antimycotic solution, 5 mL of 200 mM L-Glutamine, and 10% (v/v) fetal bovine serum. NIH3T3 cells were purchased from the American Type Culture Collection (Manassas, Virginia, USA) and cultured in high glucose Dulbecco's Modified Eagle Medium (DMEM; Thermo Fisher Scientific; 11965092) supplemented with 10% (v/v) fetal bovine serum (Atlanta Biologicals; S22660), 5 mL of 10 units/L penicillin, and 5 mL 10 mg/mL streptomycin (Thermo Fisher Scientific; 15140122). Ascorbic acid, which is an essential factor for collagen biosynthesis¹⁰⁰, was added to culture media for both cells. Prior to seeding CFs, all culture vessels were pre-coated with a gelatin-based coating solution (Cell Biologics; 6950) for one hour. Both cell lines were maintained under standard conditions of 5% CO₂ at 37 °C and 95% humidity.

Assessment of cell viability of fibroblasts treated with DOX

Cell viability of fibroblast cell lines treated with DOX were assessed by alamarBlue assay (Thermo Fisher Scientific; A50100) at a seeding density of 1 \times 10⁴ cells per well (100 μ L) in 96-well flat bottom plates. The cells were treated with a series of DOX concentrations ranging from 0 to 50 μ M for 24 h. After 21 h, 10 μ L of 10X alamarBlue was added to each well, and incubated for three hours. Fluorescence conversion was measured using a Synergy H1 microplate reader (Biotek) with 560 nm excitation and 590 nm emission.

Protein expression analysis by western blot

NIH3T3 and CFs were seeded at a density of 2 \times 10⁵ cells per well in 6-well plates one day prior to their treatments. Treatments were administered for 24 h, except for the SMAD2 phosphorylation study, which lasted for one hour. Cells were treated with DOX (1 μ M; 0.25, 1, and 2.5 μ M for CCN2 study) and 5 ng/mL TGF- β 1 or the respective vehicle control, DMSO and 4 mM HCl, respectively. ECM synthesis was promoted with 100 μ g/mL ascorbic acid during treatments¹⁰¹. Cellular proteins were extracted using radioimmunoprecipitation assay (RIPA) buffer (Thermo Fisher Scientific; 89901) containing Halt™ protease and phosphatase inhibitors (Thermo Fisher Scientific; 78442). Protein concentration in the cell lysates were determined using a Pierce™ BCA protein assay kit (Thermo Fisher Scientific; 23225).

Protein samples (30 μ g) were prepared with 4X protein sample loading buffer (LI-COR; 928-40004), and loaded onto 4–12% NuPAGE™ Bis–Tris gels (Thermo Fisher Scientific; NP0321BOX). The proteins were transferred onto pre-activated polyvinylidene difluoride (PVDF) membranes (Thermo Fisher Scientific; IB24001) using the iBlot™ 2 gel transfer device (Thermo Fisher Scientific; IB21002) with the following stepwise conditions: (1) 20 V, 1 mA, 1 min, (2) 23 V, 1 mA, 4 min, and (3) 25 V, 1 mA, 2 min. The membranes were blocked in Intercept® (tris-buffered saline; TBS) blocking buffer (LI-COR, 927-60003) for one hour and incubated with primary antibodies (protein of interest and housekeeping primary antibody tandemly) prepared in Intercept® T20 (TBS) antibody diluent (LI-COR, 927-65001) at 4 °C overnight. After overnight incubation with the primary antibody, membranes were washed and incubated with secondary antibody for one hour then washed again. Infrared detection of antibody binding on the membranes were scanned on the LI-COR Bioscience Odyssey CLX imaging system and analyzed for densitometry using LI-COR ImageStudio software.

Primary and secondary antibodies

Primary antibodies used in this study were: recombinant rabbit anti-cellular communication network factor 2 (CCN2) monoclonal antibody diluted to a concentration of 1:1,000 (Abcam, ab209780); rabbit anti-bone morphogenetic protein 1 (BMP1) polyclonal antibody diluted to a concentration of 1:1,000 (Thermo Fisher Scientific; PA5-103,660; RRID: AB_2852994); rabbit anti-collagen type I (COL1) polyclonal antibody diluted to a concentration of 1:1,000 (Thermo Fisher Scientific; PA1-26204; RRID: AB_2260734); rabbit anti-suppressors of mothers against decapentaplegic homolog 2 (SMAD2) polyclonal antibody diluted to a concentration of 1:1,000 (Thermo Fisher Scientific; 51-1300; RRID: AB_2533896); rabbit anti-phosphorylated SMAD2 (pSMAD2) monoclonal antibody diluted to a concentration of 1:1,000 (Thermo Fisher Scientific; MA5-15122; RRID: AB_10978317); and mouse anti-beta actin (β -actin) monoclonal antibody diluted to a concentration of 1:5,000 (Thermo Fisher Scientific; MA1-91399; RRID: AB_2273656).

For near-infrared fluorescence detection, IRDye® 800CW donkey anti-rabbit and IRDye® 680RD donkey anti-mouse secondary antibodies (LI-COR, 926-32213 and 926-68072, respectively) were used.

Gene expression analysis by qRT-PCR

Both cell lines were seeded at a density of 2×10^5 cells per well in 6 well plates. After one day, the cells were treated with 5 ng/mL TGF- β 1, 100 μ g/mL ascorbic acid, 1 μ M DOX or their vehicle controls for 24 h. Total RNA was extracted from the cell lines using the RNeasy Mini Kit (Qiagen; 217004). RNA concentrations were measured using a NanoDrop 2000 spectrophotometer (Thermo Fisher Scientific; ND2000USCAN). Subsequently, the RT² first strand kit (Qiagen; 330401) was utilized to perform reverse transcription of 100 ng RNA from each sample into cDNA, in accordance with the manufacturer's instructions. The cDNA was mixed with SYBR Green master-mix (Qiagen; 330503) for fluorescence detection using a thermocycler (LightCycler 96, Roche). We employed a TGF- β /BMP signaling pathway RT² Profiler™ PCR 96 well plate containing primers specific for genes related to the TGF- β /BMP signaling cascade, RNA controls, and housekeeping genes (Qiagen; PAMM-035ZF-12; 330231). The 96-well plate was loaded with 25 μ L of cDNA per well. The following thermal profile was applied: 1 cycle at 95 °C for 10 min and 45 cycles at 95 °C for 15 s, then 60 °C for one minute. A web-based tool from Qiagen, RT² Profiler PCR Data Analysis, was used for differential gene expression analysis.

Statistical analysis

The values were presented as mean \pm SE. Differences between the two groups were evaluated using the Student t-test. Differences among multiple groups were evaluated using a two-way analysis of variance (ANOVA) with Dunnett's test. The level of significance was selected to be $P < 0.05$. R statistics software was used to perform the statistical analysis.

Data availability

The authors confirm that the data supporting the findings of this study are available within the article and its supplementary materials.

Received: 19 July 2023; Accepted: 30 October 2023

Published online: 02 November 2023

References

- Zhang, S. *et al.* Identification of the molecular basis of doxorubicin-induced cardiotoxicity. *Nat. Med.* **18**, 1639–1642 (2012).
- Weaver, K. E. *et al.* Cardiovascular risk factors among long-term survivors of breast, prostate, colorectal, and gynecologic cancers: A gap in survivorship care?. *J. Cancer Surviv.* **7**, 253–261 (2013).
- Aleman, B. M. P. *et al.* Cardiovascular disease after cancer therapy. *EJC Suppl.* **12**, 18–28 (2014).
- Giza, D. E., Iliescu, G., Hassan, S., Marmagiolis, K. & Iliescu, C. Cancer as a risk factor for cardiovascular disease. *Curr. Oncol. Rep.* **19**, 1 (2017).
- Doxorubicin Hydrochloride - NCI. <https://www.cancer.gov/about-cancer/treatment/drugs/doxorubicinhydrochloride>.
- Mancilla, T. R., Davis, L. R. & Aune, G. J. Doxorubicin-induced p53 interferes with mitophagy in cardiac fibroblasts. *PLoS One* **15**, 1–27 (2020).
- Narikawa, M. *et al.* Doxorubicin induces trans-differentiation and MMP1 expression in cardiac fibroblasts via cell death-independent pathways. *PLoS One* **14**, 1–17 (2019).
- De Angelis, A. *et al.* Doxorubicin cardiotoxicity and target cells: A broader perspective. *Cardio-Oncology* **2**, 2 (2016).
- McGowan, J. V. *et al.* Anthracycline chemotherapy and cardiotoxicity. *Cardiovasc. Drugs Ther.* **31**, 63–75 (2017).
- Sampaio, D. P. S., Silva, J. B. M., do Carmo Rassi, D., Freitas, A. F. & Rassi, S. Echocardiographic strategy for early detection of cardiotoxicity of doxorubicin: A prospective observational study. *Cardio-Oncology* **8**, 1–9 (2022).
- Dobson, R. *et al.* BSE and BCOS guideline for transthoracic echocardiographic assessment of adult cancer patients receiving anthracyclines and/or trastuzumab. *JACC CardioOncol.* **3**, 1–16 (2021).
- Tak, T., Jaekel, C. M., Gharacholou, S. M., Dworak, M. W. & Marshall, S. A. Measurement of ejection fraction by cardiac magnetic resonance imaging and echocardiography to monitor doxorubicin-induced cardiotoxicity. *Int. J. Angiol.* **29**, 45–51 (2020).
- Zamorano, J. L. *et al.* 2016 ESC Position Paper on cancer treatments and cardiovascular toxicity developed under the auspices of the ESC Committee for Practice Guidelines: The Task Force for cancer treatments and cardiovascular toxicity of the European Society of Cardiology (ESC). *Eur. J. Heart Fail.* **19**, 9–42 (2017).
- Plana, J. C. *et al.* Expert consensus for multimodality imaging evaluation of adult patients during and after cancer therapy: A report from the American Society of Echocardiography and the European Association of Cardiovascular Imaging. *J. Am. Soc. Echocardiogr.* **27**, 911–939 (2014).
- Thavendiranathan, P. *et al.* Reproducibility of echocardiographic techniques for sequential assessment of left ventricular ejection fraction and volumes: Application to patients undergoing cancer chemotherapy. *J. Am. Coll. Cardiol.* **61**, 77–84 (2013).
- Martín, M. *et al.* Minimizing cardiotoxicity while optimizing treatment efficacy with trastuzumab: Review and expert recommendations. *Oncologist* **14**, 1–11 (2009).
- Steinherz, L. J., Steinherz, P. G., Tan, C. T. C., Heller, G. & Murphy, M. L. Cardiac toxicity 4 to 20 years after completing anthracycline therapy. *JAMA* **266**, 1672–1677 (1991).
- Curigliano, G. *et al.* Cardiotoxicity of anticancer treatments: Epidemiology, detection, and management. *CA Cancer J. Clin.* **66**, 309–325 (2016).
- Howlader, N. *et al.* Improved estimates of cancer-specific survival rates from population-based data. *J. Natl. Cancer Inst.* **102**, 1584–1598 (2010).
- Wouters, K. A., Kremer, L. C. M., Miller, T. L., Herman, E. H. & Lipshultz, S. E. Protecting against anthracycline-induced myocardial damage: A review of the most promising strategies. *Br. J. Haematol.* **131**, 561–578 (2005).
- Martin, M. *et al.* Adjuvant docetaxel for node-positive breast cancer. *N Engl. J. Med.* **352**, 2302–2313 (2005).
- Barrett-Lee, P. J. *et al.* Expert opinion on the use of anthracyclines in patients with advanced breast cancer at cardiac risk. *Ann. Oncol.* **20**, 816–827 (2009).
- Swain, S. M., Whaley, F. S. & Ewer, M. S. Congestive heart failure in patients treated with doxorubicin: a retrospective analysis of three trials. *Cancer* **97**, 2869–2879 (2003).

24. Goto, S. *et al.* Doxorubicin-induced DNA intercalation and scavenging by nuclear glutathione S-transferase pi. *FASEB J.* **15**, 2702–2714 (2001).
25. Yao, F. *et al.* Nanopore single-molecule analysis of DNA-doxorubicin interactions. *Anal. Chem.* **87**, 338–342 (2015).
26. Agudelo, D., Bourassa, P., Bérubé, G. & Tajmir-Riahi, H. A. Intercalation of antitumor drug doxorubicin and its analogue by DNA duplex: Structural features and biological implications. *Int. J. Biol. Macromol.* **66**, 144–150 (2014).
27. Mobaraki, M. *et al.* Molecular mechanisms of cardiotoxicity: A review on major side-effect of doxorubicin. *Indian J. Pharm. Sci.* **79**, 335–344 (2017).
28. Ramachandran, C., Samy, T. S. A., Huang, X. L., Yuan, Z. K. & Krishan, A. Doxorubicin-induced DNA breaks, topoisomerase II activity and gene expression in human melanoma cells. *Biochem. Pharmacol.* **45**, 1367–1371 (1993).
29. Bodley, A. *et al.* DNA Topoisomerase II-mediated Interaction of Doxorubicin and Daunorubicin Congeners with DNA1. *Cancer Res* 5969–5978 (1989).
30. Xie, Z., Xia, W. & Hou, M. Long intergenic non-coding RNA-p21 mediates cardiac senescence via the Wnt/ β -catenin signaling pathway in doxorubicin-induced cardiotoxicity. *Mol. Med. Rep.* **17**, 2695–2704 (2018).
31. Mitry, M. A. *et al.* Accelerated cardiomyocyte senescence contributes to late-onset doxorubicin-induced cardiotoxicity. *Am. J. Physiol. Cell Physiol.* **318**, C380–C391 (2020).
32. Marino Gammazza, A. *et al.* Doxorubicin anti-tumor mechanisms include Hsp60 post-translational modifications leading to the Hsp60/p53 complex dissociation and instauration of replicative senescence. *Cancer Lett.* **385**, 75–86 (2017).
33. Bientinesi, E. *et al.* Doxorubicin-induced senescence in normal fibroblasts promotes in vitro tumour cell growth and invasiveness: The role of Quercetin in modulating these processes. *Mech. Ageing Dev.* **206**, 111689 (2022).
34. Tatar, C., Avci, C. B., Acikgoz, E. & Oktem, G. Doxorubicin-induced senescence promotes resistance to cell death by modulating genes associated with apoptotic and necrotic pathways in prostate cancer DU145 CD133+/CD44+ cells. *Biochem. Biophys. Res. Commun.* **680**, 194–210 (2023).
35. Maejima, Y., Adachi, S., Ito, H., Hirao, K. & Isobe, M. Induction of premature senescence in cardiomyocytes by doxorubicin as a novel mechanism of myocardial damage. *Ageing Cell* **7**, 125–136 (2008).
36. Davies, K. J. A., Doroshow, J. H. & Hochstein, P. Mitochondrial NADH dehydrogenase-catalyzed oxygen radical production by adriamycin, and the relative inactivity of 5-iminodaunorubicin. *FEBS Lett.* **153**, 227–230 (1983).
37. Mukhopadhyay, P., Rajesh, M., Yoshihiro, K., Haskó, G. & Pacher, P. Simple quantitative detection of mitochondrial superoxide production in live cells. *Biochem. Biophys. Res. Commun.* **358**, 203 (2007).
38. Wu, J. *et al.* Calcium overload or underload? The effects of doxorubicin on the calcium dynamics in guinea pig hearts. *Biomedicines* **10**, 1 (2022).
39. Ondrias, K., Borgatta, L., Kim, D. H. & Ehrlich, B. E. Biphasic effects of doxorubicin on the calcium release channel from sarcoplasmic reticulum of cardiac muscle. *Circ. Res.* **67**, 1167–1174 (1990).
40. Šimůnek, T. *et al.* Anthracycline-induced cardiotoxicity: Overview of studies examining the roles of oxidative stress and free cellular iron. *Pharmacol. Rep.* **61**, 154–171 (2009).
41. Rao, V. A. Iron chelators with topoisomerase-inhibitory activity and their anticancer applications. *Antioxid. Redox. Signal* **18**, 930 (2013).
42. Wei, S. *et al.* Involvement of ROS/NLRP3 inflammasome signaling pathway in doxorubicin-induced cardiotoxicity. *Cardiovasc. Toxicol.* **20**, 507–519 (2020).
43. Shi, S., Chen, Y., Luo, Z., Nie, G. & Dai, Y. Role of oxidative stress and inflammation-related signaling pathways in doxorubicin-induced cardiomyopathy. *Cell Commun. Signal.* **21**, 1–20 (2023).
44. Reuter, S., Gupta, S. C., Chaturvedi, M. M. & Aggarwal, B. B. Oxidative stress, inflammation, and cancer: How are they linked?. *Free Radic. Biol. Med.* **49**, 1603–1616 (2010).
45. Fang, J., Seki, T. & Maeda, H. Therapeutic strategies by modulating oxygen stress in cancer and inflammation. *Adv. Drug Deliv. Rev.* **61**, 290–302 (2009).
46. Sangweni, N. F. *et al.* Prevention of anthracycline-induced cardiotoxicity: The good and bad of current and alternative therapies. *Front. Cardiovasc. Med.* **9**, 1 (2022).
47. Zhou, P. & Pu, W. T. Recounting cardiac cellular composition. *Circ. Res.* **118**, 368–370 (2016).
48. Tyaci, S. C. *et al.* Extracellular matrix regulation of metalloproteinase and antiproteinase in human heart fibroblast cells. *J. Cell Physiol.* **167**, 137–147 (1996).
49. Turner, N. A. & Porter, K. E. Regulation of myocardial matrix metalloproteinase expression and activity by cardiac fibroblasts. *IUBMB Life* **64**, 143–150 (2012).
50. Philips, N., Bashey, R. I. & Jimenez, S. A. Collagen and fibronectin expression in cardiac fibroblasts from hypertensive rats. *Cardiovasc. Res.* **28**, 1342–1347 (1994).
51. Eghbali, M. & Weber, K. T. Collagen and the myocardium: Fibrillar structure, biosynthesis and degradation in relation to hypertrophy and its regression. *Mol Cell Biochem.* **96**, 1–14 (1990).
52. Bagchi, R. A., Lin, J., Wang, R. & Czubyry, M. P. Regulation of fibronectin gene expression in cardiac fibroblasts by scleraxis. *Cell Tissue Res.* **366**, 381–391 (2016).
53. Frangiannis, N. G. Transforming growth factor- β in tissue fibrosis. *J. Experim. Med.* **217**, 1. https://doi.org/10.1084/jem_20190103 (2020).
54. Saadat, S. *et al.* Pivotal role of TGF- β /Smad signaling in cardiac fibrosis: Non-coding RNAs as effectual players. *Front. Cardiovasc. Med.* **7**, 1. <https://doi.org/10.3389/fcvm.2020.588347> (2021).
55. Leask, A. TGF β , cardiac fibroblasts, and the fibrotic response. *Cardiovasc. Res.* **74**, 207–212 (2007).
56. Travers, J. G., Kamal, F. A., Robbins, J., Yutzey, K. E. & Blaxall, B. C. Cardiac fibrosis. *Circ. Res.* **118**, 1021–1040 (2016).
57. Baudino, T. A., Carver, W., Giles, W. & Borg, T. K. Cardiac fibroblasts: Friend or foe?. *Am. J. Physiol. Heart Circ. Physiol.* **291**, 1015–1026 (2006).
58. Cleutjens, J. P. M., Verluyten, M. J. A., Smits, J. F. M. & Daemen, M. J. A. P. Collagen remodeling after myocardial infarction in the rat heart. *Am. J. Pathol.* **147**, 325 (1995).
59. Cohn, J. N., Ferrari, R. & Sharpe, N. Cardiac remodeling—Concepts and clinical implications: A consensus paper from an international forum on cardiac remodeling. *J. Am. Coll. Cardiol.* **35**, 569–582 (2000).
60. Pierreux, C. E., Nicolás, F. J. & Hill, C. S. Transforming growth factor β -independent shuttling of Smad4 between the cytoplasm and nucleus. *Mol. Cell Biol.* **20**, 9041–9054 (2000).
61. Albers, R. E., Selesniemi, K., Natale, D. R. C. & Brown, T. L. TGF- β induces Smad2 phosphorylation, ARE induction, and trophoblast differentiation. *Int. J. Stem Cells* **11**, 111 (2018).
62. Rienks, M., Papageorgiou, A.-P., Frangiannis, N. G. & Heymans, S. Myocardial extracellular matrix: An ever-changing and diverse entity. *Circ. Res.* **114**, 872–888 (2014).
63. Brown, L. Cardiac extracellular matrix: A dynamic entity. *AJP Heart Circ. Physiol.* **289**, H973–H974 (2005).
64. Ramazani, Y. *et al.* Connective tissue growth factor (CTGF) from basics to clinics. *Matrix Biol.* **68–69**, 44–66 (2018).
65. Rebollo, D. L., Lipson, K. E. & Brandan, E. Driving fibrosis in neuromuscular diseases: Role and regulation of Connective tissue growth factor (CCN2/CTGF). *Matrix Biol. Plus* **11**, 100059 (2021).
66. Chen, M. M., Lam, A., Abraham, J. A., Schreiner, G. F. & Joly, A. H. CTGF expression is induced by TGF- β in cardiac fibroblasts and cardiac myocytes: A potential role in heart fibrosis. *J. Mol Cell Cardiol* **32**, 1805–1819 (2000).

67. Gressner, O. A., Lahme, B., Demirci, I., Gressner, A. M. & Weiskirchen, R. Differential effects of TGF- β on connective tissue growth factor (CTGF/CCN2) expression in hepatic stellate cells and hepatocytes. *J. Hepatol.* **47**, 699–710 (2007).
68. Brigstock, D. R. *The CCN Family: A New Stimulus Package.* *J. Endocrinol.* **178** <http://www.endocrinology.org> (2003).
69. Pi, L. *et al.* Connective tissue growth factor with a novel fibronectin binding site promotes cell adhesion and migration during rat oval cell activation. *Hepatology* **47**, 996–1004 (2008).
70. Chen, Z. *et al.* Connective tissue growth factor: From molecular understandings to drug discovery. *Front. Cell Dev. Biol.* **8**, 1239 (2020).
71. Lipson, K. E., Wong, C., Teng, Y. & Spong, S. CTGF is a central mediator of tissue remodeling and fibrosis and its inhibition can reverse the process of fibrosis. *Fibrogen. Tiss. Repair* **5**, S24 (2012).
72. Robert Li, Y., Traore, K. & Zhu, H. Novel molecular mechanisms of doxorubicin cardiotoxicity: Latest leading-edge advances and clinical implications. *Mol. Cell Biochem.* <https://doi.org/10.1007/s11010-023-04783-3> (2023).
73. Renu, K., Tirupathi, T. P. & Arunachalam, S. Molecular mechanism of doxorubicin-induced cardiomyopathy—An update. *Eur. J. Pharmacol.* **818**, 241–253. <https://doi.org/10.1016/j.ejphar.2017.10.043> (2018).
74. Saleh, Y., Abdelkarim, O., Herzallah, K. & Abela, G. S. Anthracycline-induced cardiotoxicity: Mechanisms of action, incidence, risk factors, prevention, and treatment. *Heart Fail. Rev.* **26**, 1159–1173. <https://doi.org/10.1007/s10741-020-09968-2> (2021).
75. Bhagat, A. & Kleinerman, E. S. Anthracycline-induced cardiotoxicity: Causes, mechanisms, and prevention. in *Advances in Experimental Medicine and Biology* vol. 1257 181–192 (Springer, 2020).
76. Bartlett, J. J., Trivedi, P. C., Yeung, P., Kienesberger, P. C. & Pulimilkunnil, T. Doxorubicin impairs cardiomyocyte viability by suppressing transcription factor EB expression and disrupting autophagy. *Biochem. J.* **473**, 3769–3789 (2016).
77. Zhou, L. *et al.* Scutellarin attenuates doxorubicin-induced oxidative stress, DNA damage, mitochondrial dysfunction, apoptosis and autophagy in H9c2 cells, cardiac fibroblasts and HUVECs. *Toxicol. Vitro* **82**, 105366 (2022).
78. Kawalec, P. *et al.* Differential impact of doxorubicin dose on cell death and autophagy pathways during acute cardiotoxicity. *Toxicol. Appl. Pharmacol.* **453**, 116210 (2022).
79. Pandey, S. *et al.* Insulin-like growth factor II receptor- α is a novel stress-inducible contributor to cardiac damage underpinning doxorubicin-induced oxidative stress and perturbed mitochondrial autophagy. *Am. J. Physiol. Cell Physiol.* **317**, C235–C243 (2019).
80. Dimitrakis, P., Romay-Ogando, M. I., Timolati, F., Suter, T. M. & Zuppinger, C. Effects of doxorubicin cancer therapy on autophagy and the ubiquitin-proteasome system in long-term cultured adult rat cardiomyocytes. *Cell Tiss. Res.* **350**, 361–372 (2012).
81. Lawrence, W. T. *et al.* Doxorubicin-induced impairment of wound healing in rats. *J. Natl. Cancer Inst.* **76**, 119–126 (1986).
82. Sasaki, T., Holeyfield, K. C. & Uitto, J. Doxorubicin-induced inhibition of prolyl hydroxylation during collagen biosynthesis in human skin fibroblast cultures: Relevance to impaired wound healing. *J. Clin. Investig.* **80**, 1735–1741 (1987).
83. Sasaki, T. The effects of basic fibroblast growth factor and doxorubicin on cultured human skin fibroblasts: Relevance to wound healing. *J. Dermatol.* **19**, 664–666 (1992).
84. Muszynska, A., Palka, J. & Gorodkiewicz, E. The mechanism of Daunorubicin-induced inhibition of prolylase activity in human skin fibroblasts and its implication to impaired collagen biosynthesis. *Experim. Toxicol. Pathol.* **52**, 149–155 (2000).
85. Amirrah, I. N. *et al.* A comprehensive review on collagen type I development of biomaterials for tissue engineering: From biosynthesis to bioscaffold. *Biomedicines* **10**, 1 (2022).
86. Wittig, C. & Szulcek, R. Extracellular matrix protein ratios in the human heart and vessels: How to distinguish pathological from physiological changes?. *Front. Physiol.* **12**, 1 (2021).
87. Massagué, J., Seoane, J. & Wotton, D. Smad transcription factors. *Genes Dev.* **19**, 2783–2810 (2005).
88. Ge, G. & Greenspan, D. S. BMP1 controls TGF β 1 activation via cleavage of latent TGF β -binding protein. *J. Cell Biol.* **175**, 111 (2006).
89. Verrecchia, F. & Mauviel, A. Transforming growth factor- β signaling through the Smad pathway: Role in extracellular matrix gene expression and regulation. *J. Investig. Dermatol.* **118**, 211–215 (2002).
90. Verginadis, I. I. *et al.* A stromal Integrated Stress Response activates perivascular cancer-associated fibroblasts to drive angiogenesis and tumour progression. *Nat. Cell Biol.* **24**, 940–953 (2022).
91. Je, Y. J. *et al.* Inhibitory role of Id1 on TGF- β -induced collagen expression in human dermal fibroblasts. *Biochem. Biophys. Res. Commun.* **444**, 81–85 (2014).
92. Jakubowiak, A. *et al.* Inhibition of the transforming growth factor β 1 signaling pathway by the AML1/ETO leukemia-associated fusion protein. *J. Biol. Chem.* **275**, 40282–40287 (2000).
93. Jiang, D., Guo, B., Lin, F., Hui, Q. & Tao, K. Effect of THBS1 on the biological function of hypertrophic scar fibroblasts. *Biomed. Res. Int.* **2020**, 1 (2020).
94. Medley, S. C., Rathnakar, B. H., Georgescu, C., Wren, J. D. & Olson, L. E. Fibroblast-specific Stat1 deletion enhances the myofibroblast phenotype during tissue repair. *Wound Repair Regen* **28**, 448–459 (2020).
95. Muto, J. *et al.* Highly concentrated trehalose induces prohealing senescence-like state in fibroblasts via CDKN1A/p21. *Commun. Biol.* **6**, 1–18 (2023).
96. Roninson, I. B. Oncogenic functions of tumour suppressor p21Waf1/Cip1/Sdi1: association with cell senescence and tumour-promoting activities of stromal fibroblasts. *Cancer Lett.* **179**, 1–14 (2002).
97. Martins, S. G., Zilhão, R., Thorsteinsdóttir, S. & Carlos, A. R. Linking oxidative stress and DNA damage to changes in the expression of extracellular matrix components. *Front. Genet.* **12**, 673002 (2021).
98. Karimian, A., Ahmadi, Y. & Yousefi, B. Multiple functions of p21 in cell cycle, apoptosis and transcriptional regulation after DNA damage. *DNA Repair (Amst)* **42**, 63–71 (2016).
99. Sun, T. *et al.* Characterization of cellular senescence in doxorubicin-induced aging mice. *Exp. Gerontol.* **163**, 111800 (2022).
100. Phillips, C. L., Combs, S. B. & Pinnell, S. R. Effects of ascorbic acid on proliferation and collagen synthesis in relation to the donor age of human dermal fibroblasts. *J. Investig. Dermatol.* **103**, 228–232 (1994).
101. Marinkovic, M. *et al.* Optimization of extracellular matrix production from human induced pluripotent stem cell-derived fibroblasts for scaffold fabrication for application in wound healing. *J. Biomed. Mater. Res. A* **109**, 1803–1811 (2021).

Acknowledgements

We acknowledge support from the Institutional Development Awards (IDeA) from the National Institute of General Medical Sciences of the National Institutes of Health under Grants #P20GM103408, P20GM109095, and 1C06RR020533. We also acknowledge support from The Biomolecular Research Center at Boise State, BSU-Biomolecular Research Center, RRID:SCR_019174, with funding from the National Science Foundation, Grants #0619793 and #0923535; the M. J. Murdock Charitable Trust; Lori and Duane Stueckle, and the Idaho State Board of Education.

Author contributions

X.P. and J.T.O. conceived the experiments. C.P. and P.L. conducted the experiments. All authors analyzed the results and reviewed the manuscript.

Competing interests

The authors declare no competing interests.

Additional information

Supplementary Information The online version contains supplementary material available at <https://doi.org/10.1038/s41598-023-46216-7>.

Correspondence and requests for materials should be addressed to X.P.

Reprints and permissions information is available at www.nature.com/reprints.

Publisher's note Springer Nature remains neutral with regard to jurisdictional claims in published maps and institutional affiliations.



Open Access This article is licensed under a Creative Commons Attribution 4.0 International License, which permits use, sharing, adaptation, distribution and reproduction in any medium or format, as long as you give appropriate credit to the original author(s) and the source, provide a link to the Creative Commons licence, and indicate if changes were made. The images or other third party material in this article are included in the article's Creative Commons licence, unless indicated otherwise in a credit line to the material. If material is not included in the article's Creative Commons licence and your intended use is not permitted by statutory regulation or exceeds the permitted use, you will need to obtain permission directly from the copyright holder. To view a copy of this licence, visit <http://creativecommons.org/licenses/by/4.0/>.

© The Author(s) 2023